Functional and Structural Brain Changes in Anti–N-Methyl-D-Aspartate Receptor Encephalitis

Carsten Finke, MD,[1,2] Ute A. Kopp, PhD,[1] Michael Scheel, MD,[3] Luisa-Maria Pech,[4] Carina Soemmer,[4] Jeremias Schlichting,[4] Frank Leypoldt, MD,[5] Alexander U. Brandt, MD,[4] Jens Wuerfel, MD,[4,6] Christian Probst, PhD,[7] Christoph J. Ploner, MD,[1] Harald Prüss, MD,[1,8] and Friedemann Paul, MD[2,4,9,10,11]

Objective: Anti–N-methyl-D-aspartate receptor (NMDAR) encephalitis is an autoimmune encephalitis with a characteristic neuropsychiatric syndrome and severe and prolonged clinical courses. In contrast, standard clinical magnetic resonance imaging (MRI) remains normal in the majority of patients. Here, we investigated structural and functional brain changes in a cohort of patients with anti-NMDAR encephalitis.
Methods: Twenty-four patients with established diagnosis of anti-NMDAR encephalitis and age- and gender-matched controls underwent neuropsychological testing and multimodal MRI, including T1w/T2w structural imaging, analysis of resting state functional connectivity, analysis of white matter using diffusion tensor imaging, and analysis of gray matter using voxel-based morphometry.
Results: Patients showed significantly reduced functional connectivity of the left and right hippocampus with the anterior default mode network. Connectivity of both hippocampi predicted memory performance in patients. Diffusion tensor imaging revealed extensive white matter changes, which were most prominent in the cingulum and which correlated with disease severity. In contrast, no differences in T1w/T2w structural imaging and gray matter morphology were observed between patients and controls.
Interpretation: Anti-NMDAR encephalitis is associated with characteristic alterations of functional connectivity and widespread changes of white matter integrity despite normal findings in routine clinical MRI. These results may help to explain the clinicoradiological paradox in anti-NMDAR encephalitis and advance the pathophysiological understanding of the disease. Correlation of imaging abnormalities with disease symptoms and severity suggests that these changes play an important role in the symptomatology of anti-NMDAR encephalitis.

ANN NEUROL 2013;74:284–296

Since its first description in 2007, anti–N-methyl-D-aspartate receptor (NMDAR) encephalitis has gained widespread attention, and the clinical spectrum of the disease is now increasingly understood.[1–3] Patients typically develop amnesia, behavioral changes, psychosis, and epileptic seizures, frequently followed by a severe stage with dyskinesias, hypoventilation, and decreased levels of consciousness necessitating intensive care

View this article online at wileyonlinelibrary.com. DOI: 10.1002/ana.23932

Received Dec 3, 2012, and in revised form Apr 24, 2013. Accepted for publication Apr 26, 2013.

Address correspondence to Dr Finke, Department of Neurology, Charité–Universitätsmedizin Berlin, Charitéplatz 1, 10117 Berlin, Germany. E-mail: carsten.finke@charite.de

From the [1]Department of Neurology, Charité–Universitätsmedizin Berlin, Berlin, Germany; [2]Berlin Center for Advanced Neuroimaging, Charité–Universitätsmedizin Berlin, Berlin, Germany; [3]Department of Neuroradiology, Charité–Universitätsmedizin Berlin, Berlin, Germany; [4]Neurocure Clinical Research Center, Charité–Universitätsmedizin Berlin, Berlin, Germany; [5]Department of Neurology, University Medical Center Hamburg Eppendorf, Hamburg, Germany; [6]Institute of Neuroradiology, University Medical Center Göttingen, Göttingen, Germany; [7]Institute for Experimental Immunology, EUROIMMUN AG, Lübeck, Germany; [8]German Center for Neurodegenerative Diseases, Berlin, Germany; [9]Experimental and Clinical Research Center, Charité–Universitätsmedizin Berlin, Berlin, Germany; [10]Clinical and Experimental Multiple Sclerosis Research Center, Charité–Universitätsmedizin Berlin, Berlin, Germany; [11]Max Delbrueck Center for Molecular Medicine, Berlin, Germany.

Additional supporting information can be found in the online version of this article.

treatment. The majority of patients have a favorable outcome, although many are left with persistent cognitive deficits, including impairment of memory, attention, and executive control.[2–4] Remarkably, clinical routine brain magnetic resonance imaging (MRI) remains normal in the majority of patients despite severe clinical courses with measures of patients with unremarkable MRIs varying between 50 and 77% in large reviews.[3,5,6] Even when present, observed MRI changes are subtle and affect a wide range of brain regions in a nonspecific way. Here, we hypothesized that multimodal MRI analyses of gray and white matter together with functional imaging can help to explain this clinicoradiological discrepancy. We combined analysis of 1mm isotropic T1w and T2w structural imaging, resting state functional connectivity, white matter integrity, and gray matter morphology. Resting state functional MRI (fMRI) is an emerging functional imaging technique that analyzes spontaneous fluctuations in the blood oxygen level-dependent (BOLD) signal.[7] Correlations of these spontaneous fluctuations can be used to analyze the functional connectivity of remote brain areas in healthy and patient populations.[8] Resting state fMRI does not require specific task demands, which renders it suitable for application in cognitively impaired patients, and can detect functional changes in the brain, even when conventional MRI shows no structural changes.[9] White matter integrity was analyzed using diffusion tensor imaging (DTI), and contribution of demyelination and axonal damage to white matter changes was assessed. Voxel-based morphometry (VBM) was applied to examine changes in gray matter morphology. Finally, we analyzed whether results of these imaging analyses were associated with performance in neuropsychological testing or disease severity.

Subjects and Methods

Subjects

Twenty-four patients with anti-NMDAR encephalitis after the acute stage of the disease were studied (21 females, age = 27.9 ± 1.6 years; Table 1). Neuropsychological performance of 7 patients[4] and positron emission tomography (PET) imaging in 1 patient[10] have previously been reported. Patients were recruited in Germany and Austria between July 2011 and July 2012 and were referred to the outpatient clinic of the Department of Neurology of Charité–Universitätsmedizin Berlin for further counseling and treatment. Diagnosis was established in all patients based on characteristic clinical presentation and detection of immunoglobulin G (IgG) NMDAR antibodies. Two experienced neurologists independently assessed patients' disease severity based on the modified Rankin scale (mRS). Detection of anti-NMDAR antibodies was performed as described previously.[11] Titers during the acute encephalitic phase and at the time of imaging are listed in Table 1. The control group comprised 24 age- and gender-matched healthy subjects without any history of neurological or psychiatric disorders (21 females, age = 28.0 ± 1.7 years). NMDAR serum antibodies were determined in 23 of 24 controls and were negative in all cases, which corresponds to the well-known absence of IgG NMDAR antibodies in >1,000 healthy and disease controls in previous studies.[1,3,5,11–13] The study was approved by the Charité–Universitätsmedizin Berlin ethics committee. All study participants gave informed written consent for research and publication.

Neuropsychological Assessment

A comprehensive test battery was used, which covered verbal and nonverbal short-term and working memory (digit span forward and backward, block tapping forward and backward, both Wechsler Memory Scale-Revised), verbal and nonverbal episodic memory (Rey Auditory Verbal Learning Test [RAVLT] and Rey-Osterrieth Complex Figure Test) and executive functions (Stroop test, computerized go/no-go test, semantic fluency), object naming (Boston Naming Test), premorbid intelligence quotient (IQ; Mehrfachwahl-Wortschatz-Intelligenztest which is equivalent to the National Adult Reading Test), and general intellectual abilities (subtest 3 from the Leistungsprüfsystem, which is equivalent to Raven's Progressive Matrices).

MRI Data Acquisition

A detailed description of the MRI protocol and MRI data analysis are available in the Supplementary Material. The following sequences were acquired on a Siemens (Erlangen, Germany) Tim Trio 3T scanner at the Berlin Center of Advanced Neuroimaging at Charité–Universitätsmedizin Berlin: (1) 3-dimensional (3D) 1mm isotropic magnetization prepared rapid acquisition gradient echo, (2) echo-planar imaging sequence for the acquisition of resting state data (acquisition time = ~10 minutes; participants were instructed to lie still with their eyes closed while remaining awake), (3) single-shot echo-planar imaging sequence for the acquisition of DTI data, (4) 3D 1mm isotropic T2-weighted sequence, and (5) 3D 1mm isotropic T2-weighted fluid-attenuated inversion recovery (FLAIR) sequence.

MRI Data Analysis

Details of the MRI analysis are described in the Supplementary Material. All analyses were performed using tools from the FMRIB (Oxford, UK) Software Library (FSL; www.fmrib.ox.ac.uk/fsl). Structural scans (1mm isotropic T1, T2, and FLAIR) were reviewed by a senior neuroradiologist and compared with results of standard clinical MRI. We refer to standard clinical MRI as anatomical MRI (eg, T1, T2, FLAIR) investigations performed during clinical workup with a typical slice thickness of 3 to 5mm.

Resting State Functional Connectivity

Resting state fMRI analysis was performed using independent component analysis (ICA) and dual regression.[14] After

TABLE 1. Patient Data

Patient	Sex	Age, yr	IgG NMDAR Antibodies				Time between First Symptoms andImaging, mo	mRS	Immunotherapy at Study Time Point	Other Therapy Such as AEDs at Study Time Point	Symptoms[a]	Standard Clinical MRI	High-Resolution Structural Imaging
			CSF Titer, Initial	Serum Titer, Initial	CSF Titer, MRIStudy	Serum Titer, MRIStudy							
1	F	36	IgG1:100[b]	IgG1:1,000[b]	IgG1:32, IgM 1:3.2	IgG1:100	26	3	None	None	Dysarthria, ataxia, rigidity, severe deficits in all cognitive domains	No WM lesions	No WM lesions
2	F	23	IgG1:10[b]	IgG1:100[b]	IgG1:10	IgG1:32	42	2	None	None	Deficits of attention, executive functions and long-term memory	No WM lesions	No WM lesions
3[c]	F	32	IgG1:32[b]	IgG1:1,000[b]	IgG1:320	Neg.	39	0	None	None	None	No WM lesions	Singular WM lesion, left parieto-occipital
4[c]	M	28	IgG1:1	IgG1:3,200, IgA 1:320	IgG1:3,2	IgG1:1	52	1	None	None	Verbal long-term memory deficit	No WM lesions	No WM lesions
5[c]	F	45	IgG1:320[b]	IgG1:100[b]	IgG1:32	Neg.	53	2	None	None	Working memory deficit, increased distractibility	No WM lesions	No WM lesions
6[c]	F	30	IgG1:3.2[b]	Neg.[b]	Neg.	Neg.	40	0	None	None	(Lack of concentration, increased fatigability)	Small WM lesions	4 small WM lesions, left insular
7[c]	F	38	IgG1:32[b]	IgG1:320[b]	IgG1:32	Neg.	66	3	None	None	Moderate to severe impairments of attention and working memory and long-term memory	Multiple WM lesions	Multiple (>20) bifrontal and left insular WM lesions
8[c]	F	26	IgG1:32[b]	Neg.[b]	Neg.	IgA 1:10	72	1	None	None	Working memory deficit	No WM lesions	3 small WM lesions, right pallidum, left insular, right frontobasal
9[c]	F	22	IgG1:32[b]	IgG1:320[b]	IgG1:32	IgG1:1,000	37	1	None	None	Verbal long-term memory deficit; relapse with severe psychiatric symptoms 6 months after participation in the study	No WM lesions	No WM lesions

TABLE 1. (Continued)

Patient	Sex	Age, yr	IgG NMDAR Antibodies				Time between First Symptoms andImaging, mo	mRS	Immunotherapy at Study Time Point	Other Therapy Such as AEDs at Study Time Point	Symptoms[a]	Standard Clinical MRI	High-Resolution Structural Imaging
			CSF Titer, Initial	Serum Titer, Initial	CSF Titer, MRIStudy	Serum Titer, MRIStudy							
10	F	19	IgG1:100, IgM 1:100	IgG1:3,200	IgG1:10	IgG1:10	25	0	None	None	None	Singular left frontal WM lesion	Singular WM lesion, left frontal horn
11	F	24	IgG1:32[b]	IgG1:320[b]	Neg.	IgG1:10	15	0	None	None	None	No WM lesions	2 small WM lesions, left frontal
12	F	19	n.d.	IgG1:320[b]	IgG1:10	Neg.	16	2	None	None	Deficits of attention and impulse control	Singular left frontal WM lesion	Singular WM lesion, left frontal horn
13	F	21	IgG1:40[b]	IgG1:100[b]	IgG1:10, IgA 1:32, IgM 1:3.2	IgG1:100, IgA 1:100	41	1	None	None	Working memory deficit	No WM lesions	Singular small WM lesion, right frontal
14	F	24	n.d.	IgGPos.[b]	IgG1:3,2	Neg.	14	0	None	None	None	No WM lesions	Right frontal horn WM hyperintensity
15	F	25	n.d.	IgG1:100[b]	IgG1:1	Neg.	20	0	None	None	None	No WM lesions	Several WM lesions, right temporal horn, left trigonal, left frontal horn, left central WM
16	F	18	IgG1:100[b]	IgG1:320[b]	n.d.	IgG1:1,000	44	1	None	None	Deficits of working memory and attention	No WM lesions	No WM lesions
17	F	22	IgGPos.[b]	IgGPos.[b]	Neg.	Neg.	33	1	None	None	Mild attention deficit	No WM lesions at admission,1 new small WM lesion 4 weeks after symptom onset	Several small WM lesions, left frontal, right frontobasal
18[c]	M	42	IgGPos.[b]	IgGPos.[b]	n.d.	Neg.[b]	11	1	None	None	Verbal long-term memory deficit	No WM lesions	No WM lesions
19	F	21	n.d.	IgGPos.[b]	IgG1:1	IgG1:32	47	2	CellCept 1,000mg/day	Lamotrigin 50mg/day	Verbal long-term memory deficit	No WM lesions	No WM lesions

TABLE 1. (Continued)

Patient	Sex	Age, yr	IgG NMDAR Antibodies				Time between First Symptoms andImaging, mo	mRS	Immunotherapy at Study Time Point	Other Therapy Such as AEDs at Study Time Point	Symptoms[a]	Standard Clinical MRI	High-Resolution Structural Imaging
			CSF Titer, Initial	Serum Titer, Initial	CSF Titer, MRIStudy	Serum Titer, MRIStudy							
20	M	33	n.d.	IgGPos.[b]	IgG1:10	IgG1:100	14	3	None	None	Moderate to severe impairments of attention, short-term memory, and executive functions	No WM lesions	2 small WM lesions, frontobasal, both sides
21	F	40	IgGPos.[b]	Neg.[b]	Neg.	Neg.	19	1	None	Keppra 3g/day	Mild deficit of executive functions	Single, transient left frontal WM lesion (not detected at follow-up)	2 small WM lesions, left frontal and left temporopolar
22	F	32	IgGPos.[b]	IgGPos.[b]	Neg.	Neg.	9	1	CellCept 2,000mg/day	Keppra 2g/day	Working memory deficit and verbal long-term memory deficit	No WM lesions	No WM lesions
23	F	18	IgG1:10, IgA 1:10, IgM 1:1	IgGPos.	IgG1:3.2, IgA 1:1	IgG1:10	42	1	Methylprednisolon 4mg/day	Valproic acid	Deficits of attention, working memory, and long-term memory	No WM lesions	No WM lesions
24	F	31	IgGPos.[b]	IgG1:32[b]	Neg.	Neg.	10	1	None	Keppra 2g/day	Mild long-term memory deficit	Transient T2 hyperintense lesions, right precentral gyrus, left postcentral gyrus, left thalamus	Singular small WM lesion, right frontal

[a]Subjective symptoms are given in parentheses.
[b]IgA and IgM not determined.
[c]Neuropsychological evaluation of Patients 3–9[4] and fluorodeoxyglucose positron emission tomography imaging of Patient 18[10] have been reported previously.
AED = antiepileptic drug; CSF = cerebrospinal fluid; F = female; Ig = immunoglobulin; M = male; MRI = magnetic resonance imaging; mRS = modified Rankin scale; n.d. = not determined; Neg. = negative; NMDAR = N-methyl-D-aspartate receptor; Pos. = NMDAR antibodies positive, titer not determined (in serum usually >1:100, in CSF >1:10); WM = white matter.

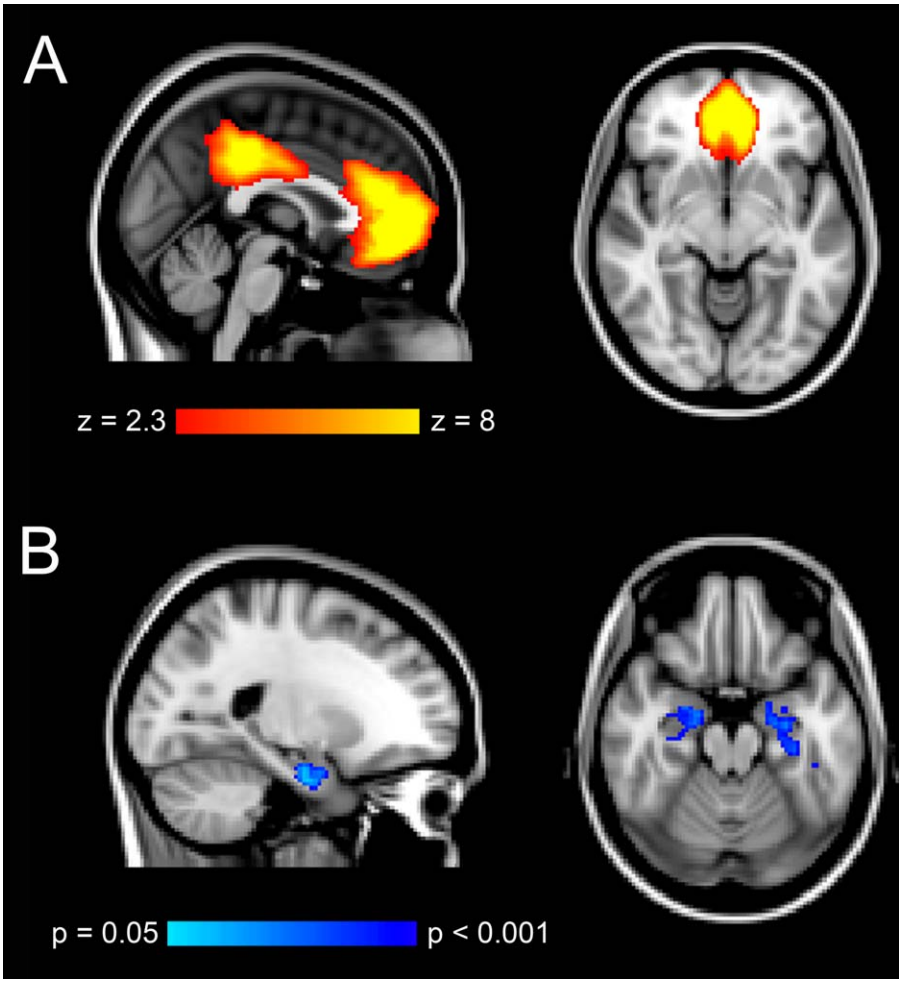

FIGURE 1: Results of resting state functional magnetic resonance imaging analysis. (A) Spatial map representing the anterior default mode network (aDMN) identified by independent component analysis. (B) Between-group analysis of resting state functional connectivity of the aDMN was performed with dual regression analysis. In patients, functional connectivity between the aDMN and both the left and the right hippocampus was significantly reduced in comparison to controls ($p < 0.05$, familywise error-corrected). [Color figure can be viewed in the online issue, which is available at www.annalsofneurology.org.]

preprocessing, resting state networks common to all subjects were identified using temporal-concatenation ICA as implemented in Multivariate Exploratory Linear Optimized Decomposition into Independent Components (MELODIC, part of FSL).[15] Analysis was focused on assessing the functional connectivity of the default mode network (DMN), as disruption of the DMN has been demonstrated in various neurological and psychiatric disorders, including Alzheimer's disease and schizophrenia, and following administration of the NMDAR antagonist ketamine.[8,9,16] Two components that captured the anterior and the posterior part of the DMN were selected for further analysis. The anterior DMN (aDMN) comprised the medial prefrontal cortex (mPFC), the anterior cingulate cortex, parts of the posterior cingulate cortex, and parts of the medial temporal lobes (MTLs; Fig 1). The posterior DMN comprised the posterior cingulate cortex, precuneus, lateral parietal cortex, parts of the ventral mPFC, and middle temporal gyri. Between-subject analysis was carried out using dual regression and nonparametric permutation testing (5,000 permutations) with threshold-free cluster enhancement (TFCE) implemented in the FSL randomize tool ($p < 0.05$, familywise error [FWE]-corrected).[14] Furthermore, we extracted functional connectivity regression coefficients from functionally defined regions of interest (ROIs) in the left and right hippocampus to run linear correlation analyses with disease severity scores and neuropsychological measures in patients.

White Matter: Diffusion Tensor Imaging

Fractional anisotropy (FA), mean diffusivity (MD), and eigenvalue maps were calculated by fitting a tensor model to the diffusion data using FMRIB's Diffusion Toolbox in FSL. Additionally, we analyzed axial diffusivity (AD) and radial diffusivity (RD), as FA is a relative parameter that is differentially influenced by these 2 values (FA increases with increasing AD and decreasing RD). AD was defined as the first eigenvalue of the diffusion tensor, and RD was calculated as the mean of the second and third eigenvalues. Voxelwise statistical analysis was carried out using tract-based spatial statistics (TBSS) and

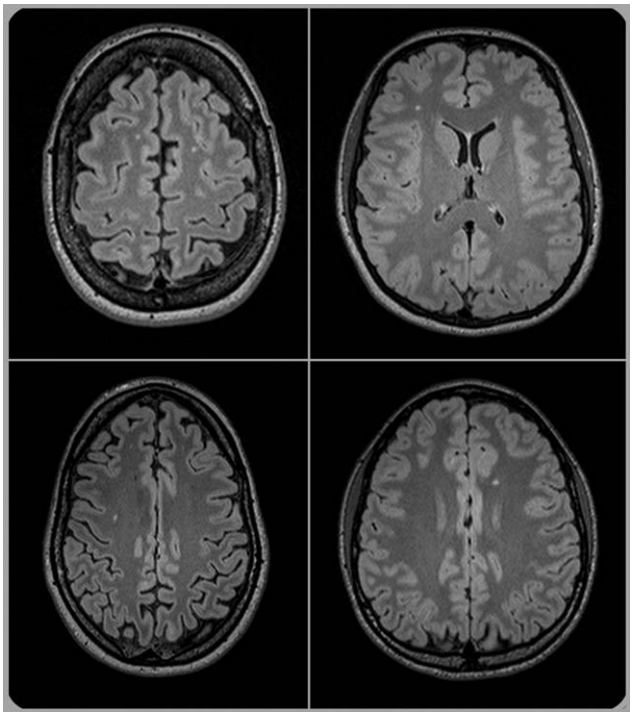

FIGURE 2: T1w and T2w 1mm isotropic structural imaging. Exemplary 3-dimensional axial fluid attenuated inversion recovery (resolution 1 × 1 × 1 mm^3) magnetic resonance images show small white matter lesions in 2 patients *(upper row)* and 2 controls *(lower row)*.

nonparametric permutation testing (5,000 permutations) with TFCE ($p < 0.05$, FWE-corrected).[17] Additionally, we performed tract-specific analysis to identify the tracts with the most prominent group differences using labels of the Johns Hopkins University DTI-based white matter atlases, which are implemented in FSL. FA group differences were tested with a linear model, and linear correlation analyses were performed to determine a possible relationship between FA values and disease severity scores.

Gray Matter: VBM

VBM analysis was performed using FSL-VBM.[18] After brain extraction and tissue-type segmentation, the resulting gray matter partial volumes images were aligned to MNI152 standard space using nonlinear registration. The resulting images were averaged to create a study-specific gray matter template. All native gray matter images were then nonlinearly reregistered to this study-specific template and modulated to correct for local expansion or contraction by dividing by the Jacobian of the warp field. The modulated gray matter images were then smoothed with an isotropic Gaussian kernel with a sigma of 3mm. Finally, voxelwise statistical analyses were performed using nonparametric permutation testing (5,000 permutations) with TFCE implemented in the FSL randomize tool ($p < 0.05$, FWE-corrected).

Hippocampal Volume

Left and right hippocampal volumes were assessed in patients and controls using the FSL tool FIRST, which performs subcortical registration and segmentation using Bayesian shape and appearance models.[19] Group differences were analyzed using 2-tailed t tests.

Results

Neuropsychological Assessment

Patients showed substantial deficits of executive functions, working memory, and verbal long-term memory, whereas attention, visuospatial abilities, and language were intact. Significant impairments were observed in the following tests: digit span backward (6.5 ± 0.4 vs 8.0 ± 0.4; Mann–Whitney test, $p = 0.008$), Stroop test (109.4 ± 4.9 vs 86.8 ± 4.3 seconds; $p = 0.001$), word fluency (26.1 ± 1.1 vs 31.4 ± 1.4; $p = 0.005$), RAVLT sum score (58.7 ± 2.1 vs 65.7 ± 1.5; $p = 0.008$), RAVLT short-term retention (12.3 ± 0.6 vs 13.8 ± 0.4; $p = 0.041$), and RAVLT recognition (13.6 ± 0.5 vs 14.7 ± 0.1; $p = 0.039$). Premorbid IQ did not differ significantly between groups (patients, 107.2 ± 2.9; controls, 114.8 ± 3.2; $p = 0.1$).

T1w/T2w Structural Imaging

3D 1mm isotropic T2 and FLAIR images demonstrated white matter lesions in 14 patients and in 8 healthy controls, the majority being small lesions (<2mm; see Table 1, Fig 2). Lesions were located predominantly within the frontal lobe without a specific pattern or configuration in patients. Only 5 patients had >2 lesions. The number of subjects with white matter lesions did not differ between the 2 groups (chi-square = 1.4, $p = 0.24$), and the number of white matter lesions did not correlate with disease severity in patients ($p = 0.25$). Of note, no white matter lesions had been detected in standard clinical MRI scans in 7 of the 14 patients with lesions now seen in the higher-resolution 3D scans. However, this is not surprising given the lower resolution of standard clinical sequences (slice thickness usually 3–5mm vs 1mm isotropic in the present study).

Resting State Functional Connectivity

Compared with controls, patients showed significantly reduced functional connectivity between the aDMN and the anterior hippocampus bilaterally (see Fig 1). To further characterize these group differences, we extracted regression coefficients from ROIs with significantly different functional connectivity in the left and right anterior hippocampus. This analysis revealed positive regression coefficients for controls, indicating coactivation of the hippocampus on both sides with the aDMN (Fig 3). Conversely, negative regression coefficients were observed in patients, demonstrating anticorrelation between hippocampal and aDMN activity. In contrast, regression coefficients for 2 control regions (frontal eye fields and dorsolateral prefrontal cortex) showed positive

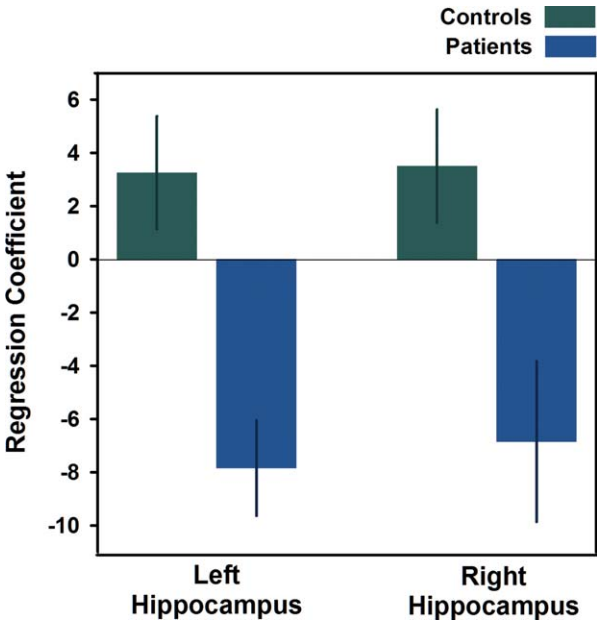

FIGURE 3: Regression coefficients of dual regression analysis for left and right anterior hippocampal regions of interest. Independent component analysis regression coefficients were extracted from functionally defined regions of interest in the anterior hippocampus. The regression coefficients represent the connectivity strength between the left/right hippocampus and the anterior default mode network (aDMN). In controls, a coactivation of the left and right anterior hippocampus with the aDMN was observed. Conversely, in patients, negative regression coefficients were observed, indicating that activity in the left and right hippocampus was anticorrelated with aDMN activity. [Color figure can be viewed in the online issue, which is available at www.annalsofneurology.org.]

values for patients and controls (Supplementary Table S1). There were no brain regions in which patients had increased functional connectivity with the aDMN relative to controls. No differences in the functional connectivity of the posterior DMN were observed between the 2 groups. To investigate the clinical relevance of the functional connectivity changes, we performed a linear correlation analysis of hippocampal regression coefficients and individual memory performance. This analysis demonstrated significant correlation between hippocampal connectivity and memory performance in patients (RAVLT sum score: left hippocampus, $r = 0.64$, $p = 0.001$; right hippocampus, $r = 0.60$, $p = 0.003$; RAVLT short-term retention: left hippocampus, $r = 0.53$, $p = 0.007$; right hippocampus, $r = 0.49$, $p = 0.016$; RAVLT delayed recall: left hippocampus, $r = 0.43$, $p = 0.034$; Supplementary Fig S1). No significant correlations of hippocampal connectivity with performance in tests of executive functions were observed. Finally, we were interested in whether hippocampal functional connectivity allows for discrimination between patients and controls. In a receiver operator characteristic (ROC) analysis, the hippocampal regression coefficients discriminated significantly between patients and controls (left hippocampus, area under the curve [AUC] $= 0.72 \pm 0.08$, $p = 0.008$; right hippocampus, AUC $= 0.72 \pm 0.08$, $p = 0.01$). To analyze whether group differences were restricted to the DMN, 3 additional networks (the sensorimotor network, primary visual network, and auditory network) were identified following the analysis of the DMN. No differences in functional connectivity were observed between patients and controls for these 3 networks (Supplementary Fig S3).

White Matter

TBSS analysis revealed widespread reduction of FA in patients relative to controls (whole skeleton, $p < 0.005$; Figs 4 and 5). No regions with significantly increased FA in patients were observed. These results were accompanied by an increase of MD in patients (whole skeleton, $p < 0.05$; see Fig 4), which was driven by an increase in RD (whole skeleton, $p < 0.008$), whereas AD values did not differ between patients and controls. Tract-specific analysis revealed that the most pronounced differences occurred in the cingulum bilaterally (Table 2). Linear correlation analysis showed significant correlation between disease severity (mRS scores) and both whole brain FA ($r = -0.53$, $p < 0.001$; Supplementary Fig S2) and FA in the cingulum (left, $r = -0.47$, $p < 0.001$; right, $r = -0.50$, $p < 0.001$), whereas no significant correlations of memory performance or executive functions with FA values were observed. In a ROC analysis, whole brain FA proved to discriminate best between patients and controls (AUC $= 0.74 \pm 0.07$, $p = 0.004$).

Gray Matter

No differences between patients and controls were observed in gray matter morphology, indicating that the altered functional connectivity in patients is unlikely to be related to structural gray matter abnormalities.

Hippocampal Volumes

Hippocampal volumes did not differ between patients and controls (left hippocampus, patients: $3{,}667 \pm 99\text{mm}^3$, controls: $3{,}860 \pm 79\text{mm}^3$, $p = 0.13$; right hippocampus, patients: $3{,}788 \pm 87\text{mm}^3$, controls: $3{,}958 \pm 95\text{mm}^3$, $p = 0.2$). Hippocampal volume did not correlate with individual memory performance in the RAVLT.

Discussion

We report the first systematic MRI investigation in anti-NMDAR encephalitis. Using resting state fMRI, we identified reduced functional connectivity of the hippocampus bilaterally that predicted memory performance in patients. Furthermore, DTI analysis revealed widespread changes in

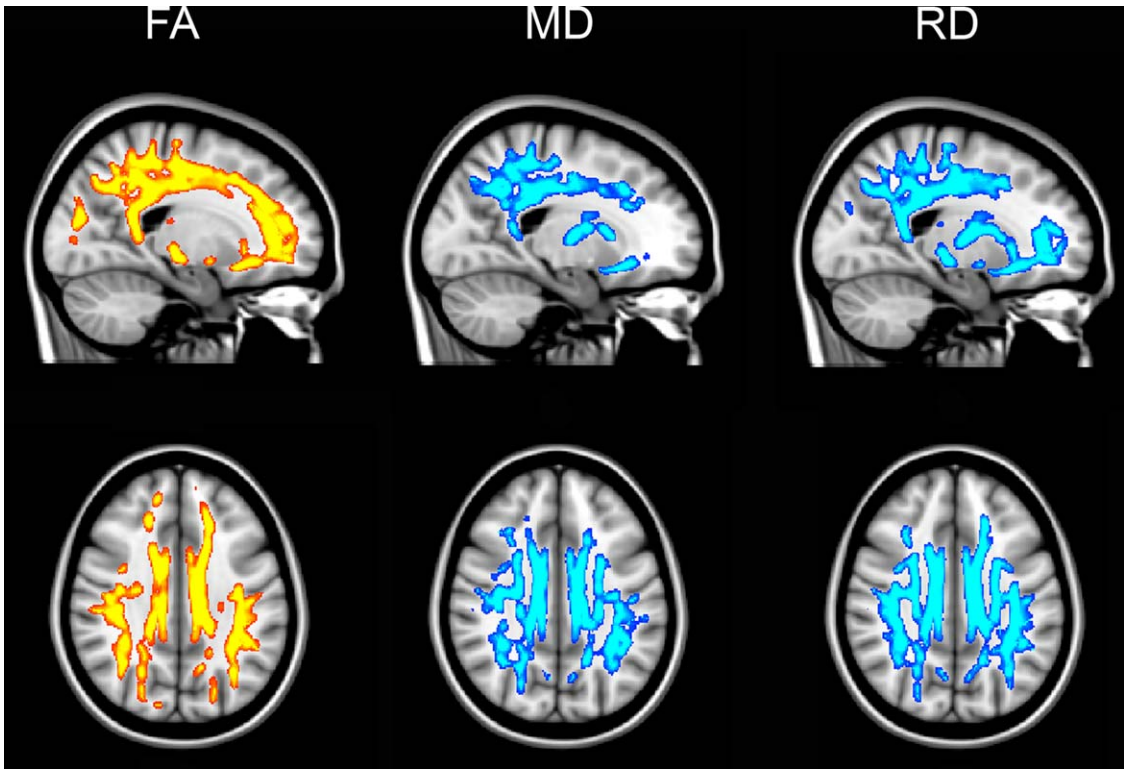

FIGURE 4: Results of tract-based spatial statistics analysis. Regions showing significant decrease of fractional anisotropy (FA), increase of mean diffusivity (MD), and/or increase of radial diffusivity (RD; $p < 0.05$, familywise error-corrected). Red/yellow voxels indicate white matter regions where FA was significantly reduced in patients relative to controls. Blue/light-blue voxels indicate white matter regions where MD and RD were significantly increased in patients relative to controls. [Color figure can be viewed in the online issue, which is available at www.annalsofneurology.org.]

white matter integrity in patients that correlated with disease severity. These results have important implications for the pathophysiological understanding and the clinical management of anti-NMDAR encephalitis.

There is a profound clinicoradiological paradox in anti-NMDAR encephalitis, with severe illness but normal brain MRI in most patients.[1–3] Standard clinical MRI was normal in the majority of patients in the present study. Unsurprisingly, we detected more small white matter lesions with 3D 1mm isotropic structural imaging that may be an indicator of vascular comorbidity. However, the number of subjects with white matter lesions did not differ significantly between patients and controls. Furthermore, the amount of white matter lesions did not correlate with disease severity in patients, and there was no specific lesion pattern in patients. Hence, even 3D 1mm isotropic structural imaging does not reveal brain changes that correspond to clinical symptoms in anti-NMDAR encephalitis patients. Further analysis of structural brain changes with VBM showed no group differences in gray matter morphology, and hippocampal volumes were not different between patients and controls. It is, however, conceivable that subtle gray matter volume reductions in hippocampal subfields might be detectable using manual methods. Furthermore, cortical DTI is an upcoming research method that has been shown to be sensitive to subtle gray matter changes and that might be able to detect alterations in gray matter that were not revealed using VBM.[20]

Using resting state fMRI, we analyzed the functional connectivity of the DMN. The DMN is a set of brain regions that decrease their activity during attention-

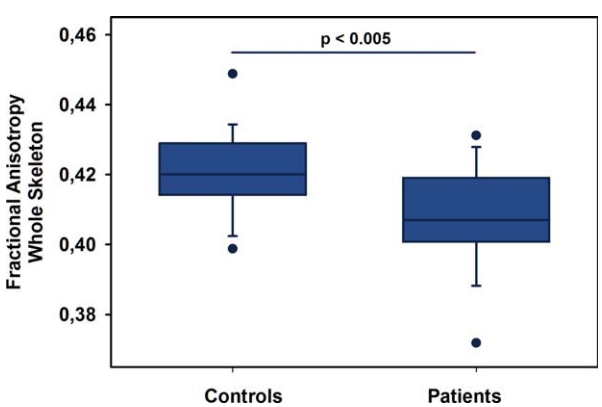

FIGURE 5: Comparison of whole skeleton fractional anisotropy between patients and controls. Whole skeleton fractional anisotropy was significantly reduced in patients with anti–N-methyl-D-aspartate receptor encephalitis in comparison to healthy controls ($p < 0.005$). [Color figure can be viewed in the online issue, which is available at www.annalsofneurology.org.]

TABLE 2. Tract-Specific FA Analysis

Tract	Controls		Patients		FA Change in %	*p*
	Mean	SD	Mean	SD		
Anterior thalamic radiation L	0.466	0.012	0.455	0.018	−2.36	0.011
Anterior thalamic radiation R	0.468	0.016	0.455	0.021	−2.78	0.029
Corticospinal tract L	0.548	0.017	0.536	0.025	−2.19	0.065
Corticospinal tract R	0.540	0.019	0.526	0.028	−2.59	0.046
Cingulum (cingulate gyrus) L	0.491	0.024	0.469	0.021	−4.48	0.002
Cingulum (cingulate gyrus) R	0.479	0.023	0.459	0.024	−4.18	0.005
Cingulum (hippocampus) L	0.424	0.033	0.405	0.033	−4.48	0.04
Cingulum (hippocampus) R	0.428	0.029	0.409	0.033	−4.44	0.051
Forceps major	0.530	0.016	0.519	0.016	−2.08	0.027
Forceps minor	0.518	0.018	0.502	0.021	−3.09	0.007
Inferior fronto-occipital fasciculus L	0.458	0.017	0.445	0.019	−2.84	0.02
Inferior fronto-occipital fasciculus R	0.464	0.018	0.449	0.019	−3.23	0.007
Inferior longitudinal fasciculus L	0.428	0.016	0.419	0.018	−2.10	0.053
Inferior longitudinal fasciculus R	0.410	0.014	0.399	0.019	−2.68	0.031
Superior longitudinal fasciculus L	0.431	0.018	0.419	0.017	−2.78	0.03
Superior longitudinal fasciculus R	0.426	0.017	0.414	0.015	−2.82	0.012
Uncinate fasciculus L	0.422	0.019	0.411	0.020	−2.61	0.054
Uncinate fasciculus R	0.435	0.027	0.418	0.022	−2.77	0.026

Tract-specific FA in patients and controls in 18 different anatomical tracts. To allow for a comparison between anatomical regions, FA reductions in patients in comparison to controls are given as percentage change. *P* values are given for independent 2-sample *t*tests (uncorrected for multiple comparisons).
FA = fractional anisotropy; L = left; R = right; SD = standard deviation.

demanding externally focused tasks and show increased activity during rest and internally directed tasks.[21] Proposed functions of the DMN include mental simulations such as envisioning the future and episodic memory processing, which are both processes that have traditionally been linked to hippocampal function.[9,22] Consequently, the hippocampus—a central component of the memory system—has been identified as part of the DMN.[9,23] Moreover, it has been shown that the DMN comprises multiple, dissociated components with a distinct MTL subsystem that is active during episodic memory processing, and that MTL activity at rest predicts individual performance in tests of memory.[24,25] Changes in DMN connectivity have been reported in several neurological and psychiatric diseases. Here, we observed a significantly reduced functional connectivity between the hippocampus and the anterior DMN in patients with anti-NMDAR encephalitis. The strength of functional connectivity correlated strongly with memory performance in patients. This observation suggests that dysfunction of hippocampal NMDAR is a central pathophysiological mechanism in anti-NMDAR encephalitis. The observation of disrupted hippocampal functional connectivity is in line with evidence that the CA1 region of the hippocampus contains the highest density of NMDAR in the brain and that loss of hippocampal NMDAR function causes severe memory deficits.[26,27] Moreover, the cognitive profile of patients with anti-NMDAR encephalitis suggests hippocampal dysfunction.[4] Direct and indirect pathways connect the hippocampus with the mPFC, a major component of the aDMN involved in executive functions and working memory.[28,29] Enhanced coactivation and oscillatory synchrony between the hippocampus and the mPFC has been observed during memory processing.[29] Hence, the reported decoupling of the hippocampus from the aDMN might explain some of the neuropsychiatric symptoms in anti-NMDAR encephalitis.

Diffusion tensor imaging revealed widespread changes of white matter integrity in patients. Whole

brain and cingulum FA values significantly correlated with disease severity, suggesting a close relationship between NMDAR antibody-mediated pathophysiology and white matter damage. Reductions in FA were driven by an increase of RD, but not a decrease in AD. This pattern has been suggested to be indicative of demyelination as opposed to axonal damage.[30] White matter changes were most prominent in the cingulum bundle, a fiber tract that connects the cingulate cortex with other components of the limbic system. It is therefore relevant for frontotemporal interaction, and damage to the cingulum has been associated with impairments of working memory and executive functions.[31] Interestingly, FA of the cingulum is closely linked to the level of DMN functional connectivity.[32] It therefore might be speculated that the reduced hippocampal–aDMN connectivity in patients is at least partially attributable to cingulum white matter damage. ROC analyses showed that both whole brain FA and hippocampal functional connectivity discriminated well between patients and controls. These results highlight the potential of both imaging analyses for the differential diagnosis of anti-NMDAR encephalitis, although larger samples sizes should be investigated to further evaluate the diagnostic accuracy in single subjects. Interestingly, widespread changes of white matter integrity that extend beyond the affected MTL have also been observed in patients with herpes encephalitis.[33] Future studies are needed to investigate the specificity of white matter damage in patients with different forms of encephalitis. These studies will likewise elucidate how imaging patterns in anti-NMDAR encephalitis compare to other types of autoimmune encephalitis. Our results also extend previous reports on brain PET abnormalities during the acute stage of anti-NMDAR encephalitis. While several case descriptions showed altered cerebral metabolic activity but did not yield a consistent pattern,[3,34,35] Leypoldt et al. observed an increased frontotemporal-occipital gradient of glucose metabolism in 6 patients.[10] Differences between these brain PET results and our findings in resting state fMRI and DTI might be related to differences in the disease stage at the time of imaging and to significant methodological differences between PET imaging and resting state fMRI.

Many of the acute clinical symptoms of anti-NMDAR encephalitis resemble those found in schizophrenia. NMDAR hypofunction is now considered a central pathophysiological mechanism in schizophrenia, and administration of the NMDAR antagonist ketamine induces symptoms common to both diseases, for example, memory impairment, thought disorder, and impairment of executive functions.[36,37] The effect of ketamine on functional connectivity of the DMN was recently investigated in healthy subjects. Ketamine induced profound disruption of DMN connectivity that correlated with working memory impairment and ketamine-induced psychiatric symptoms.[16] Likewise, schizophrenia patients show extensive alterations of DMN connectivity, including reduced functional connectivity of the hippocampus with DMN nodes.[8,9,38] Furthermore, FA changes in the cingulum bundle that were correlated with cognitive performance and clinical symptoms have repeatedly been reported in schizophrenia.[31,39] The currently reported results complement these findings by showing disruption of hippocampal–DMN connectivity and prominent cingulum white matter pathology in anti-NMDAR encephalitis, suggesting a comparable pathophysiological mechanism of anti-NMDAR encephalitis and schizophrenia. New treatment strategies that target NMDAR hypofunction might therefore prove helpful in both diseases.[36]

On a molecular level, NMDAR antibodies cause an internalization of synaptic NMDAR. It has been suggested that this decrease of NMDAR predominantly inactivates NMDAR-rich γ-aminobutyric acidergic (GABAergic) neurons, causing an increase of extracellular glutamate and a disinhibition of excitatory pathways.[2] Preferential disruption of NMDA conductance on GABAergic neurons in a computational model accounted for task-based BOLD modulations of the DMN observed after ketamine administration in healthy subjects.[16] This model parsimoniously reconciled BOLD signal reduction and working memory impairment with disinhibition, suggesting that the here reported reduced hippocampal functional connectivity might be explained within this framework. The observed white matter damage might be caused by affection of oligodendrocyte NMDARs that have recently been discovered.[40]

Our study demonstrates substantial structural and fMRI abnormalities in patients with anti-NMDAR encephalitis, whereas standard clinical MRI and high-resolution structural imaging revealed no clinically relevant brain changes. We observed extensive white matter damage and reduced hippocampal–DMN functional connectivity that correlated with disease severity and memory performance in patients. These imaging analyses therefore contribute to an improved understanding of the clinicoradiological paradox in anti-NMDAR encephalitis. Results of ROC analyses furthermore suggest that these MRI methods may become valuable tools in the diagnosis and therapy monitoring of anti-NMDAR encephalitis.

Acknowledgment

This study was supported by the German Research Council (DFG Exc 257, F.P.; DFG Pl 248/4-1, C.J.P.).

We thank all patients and healthy controls for their participation, S. Pikol and C. Kraut for help with MRI data acquisition, N. Voets for help with fMRI data analysis, and K.D. Wernecke for statistical advice.

Authorship

H.P. and F.P. contributed equally.

Potential Conflicts of Interest

M.S.: grants/grants pending, Volkswagen Stiftung and Stiftung Charité. F.L.: grants/grants pending, EUROIMMUN. A.U.B.: employment, stock/stock options, gfnmediber; grants/grants pending, Novartis Pharma; speaking fees, Heidelberg Engineering, Bayer; travel expenses, Merck Serono, Novartis Pharma. J.W.: consultancy, Novartis; grants/grants pending, Novartis, German Ministry for Science and Research; speaking fees, Bayer. C.P.: stock/stock options, EUROIMMUN. F.P.: consultancy, Novartis, OCTIMS Steering Committee; grants/-grants pending, speaking fees, Novartis, Teva, Bayer Schering, Merck Serono, Sanofi-Genzyme, Biogen Idec; travel expenses, Guthy-Jackson Charitable Foundation.

References

1. Dalmau J, Tüzün E, Wu H, et al. Paraneoplastic anti-N-methyl-D-aspartate receptor encephalitis associated with ovarian teratoma. Ann Neurol 2007;61:25–36.
2. Dalmau J, Lancaster E, Martinez-Hernandez E, et al. Clinical experience and laboratory investigations in patients with anti-NMDAR encephalitis. Lancet Neurol 2011;10:63–74.
3. Irani SR, Bera K, Waters P, et al. N-methyl-D-aspartate antibody encephalitis: temporal progression of clinical and paraclinical observations in a predominantly non-paraneoplastic disorder of both sexes. Brain 2010;133(pt 6):1655–1667.
4. Finke C, Kopp UA, Prüss H, et al. Cognitive deficits following anti-NMDA receptor encephalitis. J Neurol Neurosurg Psychiatry 2012; 83:195–198.
5. Dalmau J, Gleichman AJ, Hughes EG, et al. Anti-NMDA-receptor encephalitis: case series and analysis of the effects of antibodies. Lancet Neurol 2008;7:1091–1098.
6. Titulaer MJ, McCracken L, Gabilondo I, et al. Treatment and prognostic factors for long-term outcome in patients with anti-NMDA receptor encephalitis: an observational cohort study. Lancet Neurol 2013;4422:1–9.
7. Fox MD, Raichle ME. Spontaneous fluctuations in brain activity observed with functional magnetic resonance imaging. Nat Rev Neurosci 2007;8:700–711.
8. Zhang D, Raichle ME. Disease and the brain's dark energy. Nat Rev Neurol 2010;6:15–28.
9. Buckner RL, Andrews-Hanna JR, Schacter DL. The brain's default network: anatomy, function, and relevance to disease. Ann N Y Acad Sci 2008;1124:1–38.
10. Leypoldt F, Buchert R, Kleiter I, et al. Fluorodeoxyglucose positron emission tomography in anti-N-methyl-D-aspartate receptor encephalitis: distinct pattern of disease. J Neurol Neurosurg Psychiatry 2012;83:681–686.
11. Wandinger K-P, Saschenbrecker S, Stoecker W, Dalmau J. Anti-NMDA-receptor encephalitis: a severe, multistage, treatable disorder presenting with psychosis. J Neuroimmunol 2011;231:86–91.
12. Steiner J, Walter M, Glanz W, et al. Increased prevalence of diverse N-methyl-D-aspartate glutamate receptor antibodies in patients with an initial diagnosis of schizophrenia: specific relevance of IgG NR1a antibodies for distinction from N-methyl-D-aspartate glutamate receptor encephalitis. JAMA Psychiatry 2013; 70:271–278.
13. Prüss H, Höltje M, Maier N, et al. IgA NMDA receptor antibodies are markers of synaptic immunity in slow cognitive impairment. Neurology 2012;78:1743–1753.
14. Filippini N, MacIntosh BJ, Hough MG, et al. Distinct patterns of brain activity in young carriers of the APOE-epsilon4 allele. Proc Natl Acad Sci U S A 2009;106:7209–7214.
15. Beckmann CF, DeLuca M, Devlin JT, Smith SM. Investigations into resting-state connectivity using independent component analysis. Philos Trans R Soc Lond B Biol Sci 2005;360:1001–1013.
16. Anticevic A, Gancsos M, Murray JD, et al. NMDA receptor function in large-scale anticorrelated neural systems with implications for cognition and schizophrenia. Proc Natl Acad Sci U S A 2012; 109:16720–16725.
17. Smith SM, Jenkinson M, Johansen-Berg H, et al. Tract-based spatial statistics: voxelwise analysis of multi-subject diffusion data. Neuroimage 2006;31:1487–1505.
18. Ashburner J, Friston KJ. Voxel-based morphometry—the methods. Neuroimage 2000;11(6 pt 1):805–821.
19. Patenaude B, Smith SM, Kennedy DN, Jenkinson M. A Bayesian model of shape and appearance for subcortical brain segmentation. Neuroimage 2011;56:907–922.
20. Oreja-Guevara C, Rovaris M, Iannucci G, et al. Progressive gray matter damage in patients with relapsing-remitting multiple sclerosis: a longitudinal diffusion tensor magnetic resonance imaging study. Arch Neurol 2005;62:578–584.
21. Raichle ME, MacLeod AM, Snyder AZ, et al. A default mode of brain function. Proc Natl Acad Sci U S A 2001;98:676–682.
22. Martin VC, Schacter DL, Corballis MC, Addis DR. A role for the hippocampus in encoding simulations of future events. Proc Natl Acad Sci U S A 2011;108:13858–13863.
23. Greicius MD, Srivastava G, Reiss AL, Menon V. Default-mode network activity distinguishes Alzheimer's disease from healthy aging: evidence from functional MRI. Proc Natl Acad Sci U S A 2004;101: 4637–4642.
24. Andrews-Hanna JR, Reidler JS, Sepulcre J, et al. Functional-anatomic fractionation of the brain's default network. Neuron 2010; 65:550–562.
25. Wig GS, Grafton ST, Demos KE, et al. Medial temporal lobe BOLD activity at rest predicts individual differences in memory ability in healthy young adults. Proc Natl Acad Sci U S A 2008; 105:18555–18560.
26. Monaghan DT, Cotman CW. Distribution of N-methyl-D-aspartate-sensitive L-[3H]glutamate-binding sites in rat brain. J Neurosci 1985;5:2909–2919.
27. Nakazawa K, McHugh TJ, Wilson MA, Tonegawa S. NMDA receptors, place cells and hippocampal spatial memory. Nat Rev Neurosci 2004;5:361–372.
28. Miller EK, Cohen JD. An integrative theory of prefrontal cortex function. Annu Rev Neurosci 2001;24:167–202.
29. Colgin LL. Oscillations and hippocampal-prefrontal synchrony. Curr Opin Neurobiol 2011;21:467–474.
30. Song S-K, Sun S-W, Ramsbottom MJ, et al. Dysmyelination revealed through MRI as increased radial (but unchanged axial) diffusion of water. Neuroimage 2002;17:1429–1436.

31. Kubicki M, Westin C-F, Nestor PG, et al. Cingulate fasciculus integrity disruption in schizophrenia: a magnetic resonance diffusion tensor imaging study. Biol Psychiatry 2003;54:1171–1180.

32. Van den Heuvel M, Mandl R, Luigjes J, Hulshoff Pol H. Microstructural organization of the cingulum tract and the level of default mode functional connectivity. J Neurosci 2008;28: 10844–10851.

33. Grydeland H, Walhovd KB, Westlye LT, et al. Amnesia following herpes simplex encephalitis: diffusion-tensor imaging uncovers reduced integrity of normal-appearing white matter. Radiology 2010;257:774–781.

34. Maeder-Ingvar M, Prior JO, Irani SR, et al. FDG-PET hyperactivity in basal ganglia correlating with clinical course in anti-NDMA-R antibodies encephalitis. J Neurol Neurosurg Psychiatry 2011;82: 235–236.

35. Iizuka T, Sakai F, Ide T, et al. Anti-NMDA receptor encephalitis in Japan: long-term outcome without tumor removal. Neurology 2008;70:504–511.

36. Moghaddam B, Javitt D. From revolution to evolution: the glutamate hypothesis of schizophrenia and its implication for treatment. Neuropsychopharmacology 2012;37:4–15.

37. Adler CM, Goldberg TE, Malhotra AK, et al. Effects of ketamine on thought disorder, working memory, and semantic memory in healthy volunteers. Biol Psychiatry 1998;43:811–816.

38. Zhou Y, Shu N, Liu Y, et al. Altered resting-state functional connectivity and anatomical connectivity of hippocampus in schizophrenia. Schizophr Res 2008;100:120–132.

39. Voineskos AN, Lobaugh NJ, Bouix S, et al. Diffusion tensor tractography findings in schizophrenia across the adult lifespan. Brain 2010;133(pt 5):1494–1504.

40. Káradóttir R, Cavelier P, Bergersen LH, Attwell D. NMDA receptors are expressed in oligodendrocytes and activated in ischaemia. Nature 2005;438:1162–1166.